Environmental Science & Technology

Subscriber access provided by University Libraries | University of Notre Dame

Article

An integrated experimental and modeling approach to predict sediment mixing from benthic burrowing behavior

Kevin R Roche, Antoine F Aubeneau, Minwei Xie, Tomás C Aquino, Diogo Bolster, and Aaron I. Packman

Environ. Sci. Technol., **Just Accepted Manuscript** • DOI: 10.1021/acs.est.6b01704 • Publication Date (Web): 16 Aug 2016

ACS Publications

Environmental Science & Technology is published by the American Chemical Society. 1155 Sixteenth Street N.W., Washington, DC 20036

An integrated experimental and modeling approach to predict sediment mixing from benthic burrowing behavior

Kevin R. Roche[*†], *Antoine F. Aubeneau*[§], *Minwei Xie*[†], *Tomás Aquino*[‡], *Diogo Bolster*[‡], *and Aaron I. Packman*[†]

[†]Department of Civil and Environmental Engineering, Northwestern University, 2145 Sheridan Road, Evanston, Illinois 60208-3109, United States

[§] Lyles School of Civil Engineering, Purdue University, 550 Stadium Mall Drive, West Lafayette, IN 47907-2051, United States

[‡]Department of Civil and Environmental Engineering and Earth Sciences, University of Notre Dame, Notre Dame, IN 46556, United States

ABSTRACT

Bioturbation is the dominant mode of sediment transport in many aquatic environments, and strongly influences both sediment biogeochemistry and contaminant fate. Available bioturbation models rely on highly simplified biodiffusion formulations that inadequately capture the behavior of many benthic organisms. We present a novel experimental and modeling approach that uses time-lapse imagery to directly relate burrow formation to resulting sediment mixing.

We paired white-light imaging of burrow formation with fluorescence imaging of tracer particle redistribution by the oligochaete *Lumbriculus variegatus*. We used the observed burrow formation statistics and organism density to parameterize a parsimonious model for sediment mixing based on fundamental random walk theory. Worms burrowed over a range of times and depths, resulting in homogenization of sediments near the sediment-water interface, rapid nonlocal transport of tracer particles to deep sediments, and large areas of unperturbed sediments. Our fundamental, parsimonious random walk model captures the central features of this highly heterogeneous sediment bioturbation, including evolution of the sediment-water interface coupled with rapid near-surface mixing, and anomalous late-time mixing resulting from infrequent deep burrowing events. This approach provides a general, transferable framework for explicitly linking sediment transport to governing biophysical processes.

INTRODUCTION

Sediment-dwelling organisms modify their local environment as they burrow, scavenge for food, and hide from predators. Biological reworking of sediments, termed *bioturbation*, mixes particles in the sediment bed[1-3]. Reworked sediments encounter different biogeochemical environments that control particle transformation, for example by microbial metabolism, precipitation/dissolution, and sorption/desorption processes. Particulate organic matter is metabolized more slowly in anoxic sediments, and particles retained in such environments are more likely to be preserved[4-6]. Similarly, reduced metal sulfides are oxidized when transported from depth into oxic surficial environments, leading to liberation of bioavailable dissolved metals[7-11]. Bioturbation is thus an important transport process that should be included in biogeochemical models for sediment diagenesis and contaminant fate in sediments.

Continuum models are widely used to represent bioturbation[12-15]. These models treat the subsurface as a continuous domain with volume-averaged bulk properties, such as porosity and particle concentrations. The simplest continuum model for bioturbation is the 1-D biodiffusion model[13, 16-19]. In this model, fluxes are proportional to local concentration gradients, following classical Fickian diffusion assumptions, yielding particle motions that are small, isotropic and frequent relative to the scale of observation[20, 21]. Scale restrictions limit the applicability of local continuum models in natural environments. Motion that violates standard assumptions of regular Fickian diffusion, and thus cannot be predicted by continuum biodiffusion models, is commonly termed *anomalous transport*[22, 23]. Fickian assumptions are violated when organisms quickly transport sediments over long distances. In this case, particle fluxes are not controlled solely by local concentration gradients, and are thus *nonlocal*. Commonly used bioturbation models are also *asymptotic*, meaning they are valid only after a large number of mixing events have been observed. However, timescales for sediment mixing by bioturbation can be very large because burrowing is highly heterogeneous and new burrow formation is infrequent, yielding substantial deviations from asymptotic model predictions[21].

Several approaches have been proposed for anomalous bioturbation. Robbins[24] and Boudreau[25] independently developed models to describe upward-conveying deposit feeders, which are worms that continuously ingest sediments at depth and egest them above the sediment-water interface (SWI). These models include a nonlocal transport term associated with feeding over a range of depths. François et al.[26] extended this approach to 2-D using a finite element numerical model. Stochastic continuous time random walk (CTRW) models have also been proposed for bioturbation[27, 28]. As with Fickian biodiffusion, CTRW models describe the ensemble redistribution of particles resulting from an underlying random motion, but no predefined range

of scales are assumed in the CTRW formulation. Instead, the model is parameterized with probability density functions (PDFs) whose shapes explicitly define the scales that govern particle movements.

A scarcity of direct observations limits identification and parameterization of bioturbation models[27, 31]. Current models assume, but do not verify, that biodiffusion and nonlocal transport are the relevant processes governing sediment mixing. Incorrect assumptions of governing processes greatly limit model fidelity and transferability, since model parameters are not clearly linked to fundamental, measurable system attributes. The goal of the present study was to develop a parsimonious model to directly relate statistics of burrow formation to resulting sediment mixing. We used *Lumbriculus variegatus* as a model organism because it is a common bioturbator of freshwater sediments and a standard test organism for contaminant transport and toxicity studies[32-34]. *L. variegatus* is a head-down deposit feeder that transports sediments nonlocally by ingesting particles at depth and egesting them at the SWI. Using time-lapse imagery, we observed the development of burrow structures and the resulting redistribution of tracer particles within experimental chambers. We then used the observed burrow statistics to parameterize a numerical random walk model for sediment bioturbation, and tested the model predictions against independent observations of sediment transport.

METHODS

Sediment Collection and Characterization

We collected sediments from Lake DePue, a shallow backwater lake of the Illinois River (IL, USA). Sediments, collected to a depth of 15 cm, were transported to the laboratory and refrigerated at 4 °C until used. Sediments were characterized by Xie et al.[35]. 81% of the

sediments by volume had a diameter ≤45 μm, and ~70% had a diameter ≤10 μm. Bulk sediment properties (porosity, permeability, carbon content, and metals concentrations) are reported in the Supporting Information.

Experimental Setup

Organism burrowing and sediment mixing were observed in an acrylic aquarium (10 cm long x 10 cm wide x 22 cm high). We added 8 cm of homogenized sediment to the aquarium and then added 1.5 L of artificially-reconstituted fresh water (see Supporting Information)[35,36], creating a 10-cm water column that was constantly recirculated between the aquarium and the reservoir. A mechanical stirrer (IKA Lab Egg, Cole Parmer, IL, USA) was used to keep the overlying water in the aquarium well mixed, and the reservoir was constantly aerated so that the water column remained oxic.

We allowed sediments to stabilize for 24 h, which was sufficient for all suspended particles to deposit back to the bed. We then added 5 mg of fluorescent tracer particles (ZQ-14, DayGlo Color Corp, OH) to form a uniform 0.8-mm-thick layer at the SWI. Tracer particles had excitation and emission wavelengths of 405 nm and 620 nm, respectively. The tracer particle size (20-60 μm in diameter) was chosen so that particle mobility was similar to Lake DePue sediments, based on the critical shear for resuspension.

We added 0.250 g of *Lumbriculus variegatus* (Aquatic Research Organisms, Hampton, NH, USA) evenly over the SWI immediately following sediment stabilization. This corresponds to an organism density of 6,300/m^2,[37] which falls within the typical range of oligochaete densities in freshwater sediments, 1,000-40,000/m^2 [38-40]. *L. variegatus* egested and excreted the organic-rich test sediments, and no exogenous food was added during the experiment.

This experimental setup enabled us to directly assess the linkage between *L. variegatus* movement and sediment transport, since all observed transport events were directly associated with organism motions. We used time-lapse photography to capture *L. variegatus* burrowing activity and resulting sediment transport. Methods to measure tracer particle motion follow those previously used to assess biological reworking of freshwater and marine sediments[28, 29]. We placed a digital camera (Nikon D7000, 40-mm macro lens) 35 cm from one face of the experimental chamber (Figure 1), providing a 13-μm pixel resolution. Burrow development and resulting sediment mixing were then imaged with a series of three photographs taken at 3-min intervals. Tracer particles were first imaged using ultraviolet LEDs (excitation wavelength 407 nm, Super Bright LEDs Inc., St. Louis, USA), and the fluorescent emission signal was isolated by a 610-nm bandpass filter (10 nm bandwidth, Edmund Optics Inc., NJ, USA). White LEDs (Super Bright LEDs) were then triggered to capture the SWI location SWI and worm burrows. Lastly, a dark image was taken to measure background light. The experiment was replicated in duplicate using sediments from the same sample and identical image-acquisition hardware.

Image Processing

Image processing, numerical simulations, and model fits were performed with Matlab R2015b (Mathworks Inc., USA). Images were converted from .RAW to .JPEG using a linear tone curve, after which background light intensity was subtracted (dark images). We quantified SWI movement by first identifying images where the SWI changed rapidly (e.g., because of sediment mound collapse). We manually traced the SWI in these images and then automatically interpolated the SWI for all others.

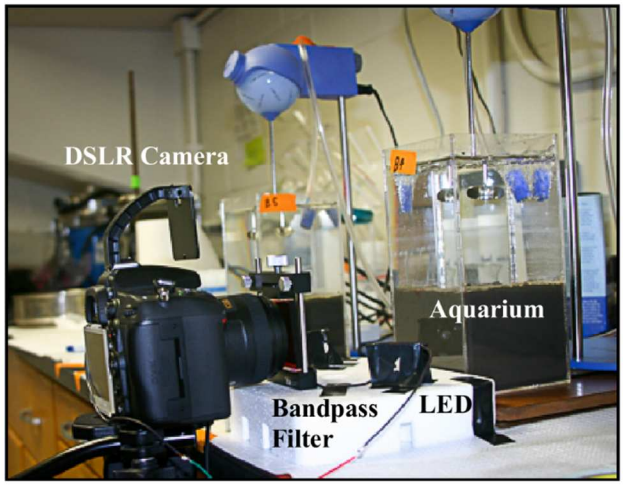

***Figure 1**: Experimental setup.*

To calculate tracer particle distributions, we averaged light intensity over the width of each fluorescent image to generate a 1-D fluorescence intensity profile, $F(x,t)$, where x = distance below the SWI and t = time since worms were added. We then normalized these profiles by the overall light intensity measured below the SWI:

$$P(x,t) = \frac{F(x,t)}{\sum_x F(x,t)}. \quad (1)$$

Burrows were identified using white-light images. We smoothed these images using a Gaussian filter and binarized them using a global thresholding algorithm (detailed in Supporting Information). Because LED intensity varied slightly from image to image, we averaged images over a 90-min window to exclude optical noise and minimize misidentification of spurious burrowing events. We then coarsened the resulting grayscale images to 230-µm pixels, corresponding to the typical burrow width. The resulting image was 205 x 137 pixels. Burrow development was determined from pixels that changed from light to dark between successive images. Burrows were identified at a threshold of <15% light intensity to minimize false positives. For each pixel that changed from light to dark, the pixel depth and the time since the last disturbance event (wait time) were recorded. We used these results to generate a joint PDF:

$$\Psi(x,\tau) = \frac{n(x,\tau)}{N} \quad (2)$$

where $\Psi(x,\tau)$ is the probability density of a burrow event occurring at depth x after wait time τ, $n(x,\tau)$ is the number of events that occurred for a pixel centered at depth x with wait time τ, and N is the total number of events. Marginal burrow-depth and wait-time PDFs were computed from the joint PDF by integrating over the complementary parameter:

$$\lambda\,(x) = \int_{\tau} \Psi(x,\tau)\,\mathrm{d}\tau \quad (3)$$

$$\varphi(\tau) = \int_{x} \Psi(x,\tau)\,\mathrm{d}x. \quad (4)$$

Random Walk Model

We constructed a numerical random walk model for sediment motion conditioned on $\Psi(x,\tau)$. The model domain consisted of a 2-D grid, identical to the coarsened grid used to monitor burrowing events. Model time steps were set equal to the averaging window for experimental images (90 min). The initial condition was a thin layer of tracer added uniformly to the top 0.8 mm of the grid, which matched the experimental conditions.

We considered two different random walk models: coupled and uncoupled. In the coupled model, sediment particles sample a wait time, T$\sim\varphi$, and then sample a burrow depth from the joint density, $X\sim\Psi(\cdot,\mathrm{T})$, which is conditioned on T. In the uncoupled model, sediment particles sample independently from φ and λ. Burrowing events are considered vertical and instantaneous, so within a single time step a worm is assumed to have burrowed and returned to the surface. The horizontal location of each burrow is randomly assigned from a uniform distribution. Tracer particles are redistributed according to a set of rules that transports a fraction of sediments to the SWI at a rate proportional to the mean SWI velocity (i.e. rate of SWI movement due to sediment

reworking), and a characteristic burrow velocity derived from the marginal PDFs (see Supporting Information).

We ran 200 realizations of the model to generate ensemble-averaged concentration profiles $C(x,t)$. Worm densities matched experimental conditions, 6,300/m^2. We then calculated the mean and variance for the tracer particle concentration profile at each time:

$$E(X,t) = \int_0^{x_{max}} xC(x,t)\mathrm{d}x \tag{5}$$

$$E(X^2,t) = \int_0^{x_{max}} \big(x - E(X,t)\big)^2 C(x,t)\mathrm{d}x. \tag{6}$$

Biodiffusion Model

For comparison, we fit a simple advection-diffusion (ADE) model to experimental results:

$$\frac{\partial C(x,t)}{\partial t} + U_b \frac{\partial C(x,t)}{\partial x} = D_b \frac{\partial^2 C(x,t)}{\partial x^2} \tag{7}$$

where U_b is the bioadvective drift of the tracer peak and D_b is the effective biodiffusion coefficient (both assumed constant). We treated the SWI as a no-flux boundary, enabling a standard Green's function solution to the problem[41]. We fit U_b and D_b with a Maximum Likelihood Estimation method[42].

177 RESULTS

178 *Burrow statistics*

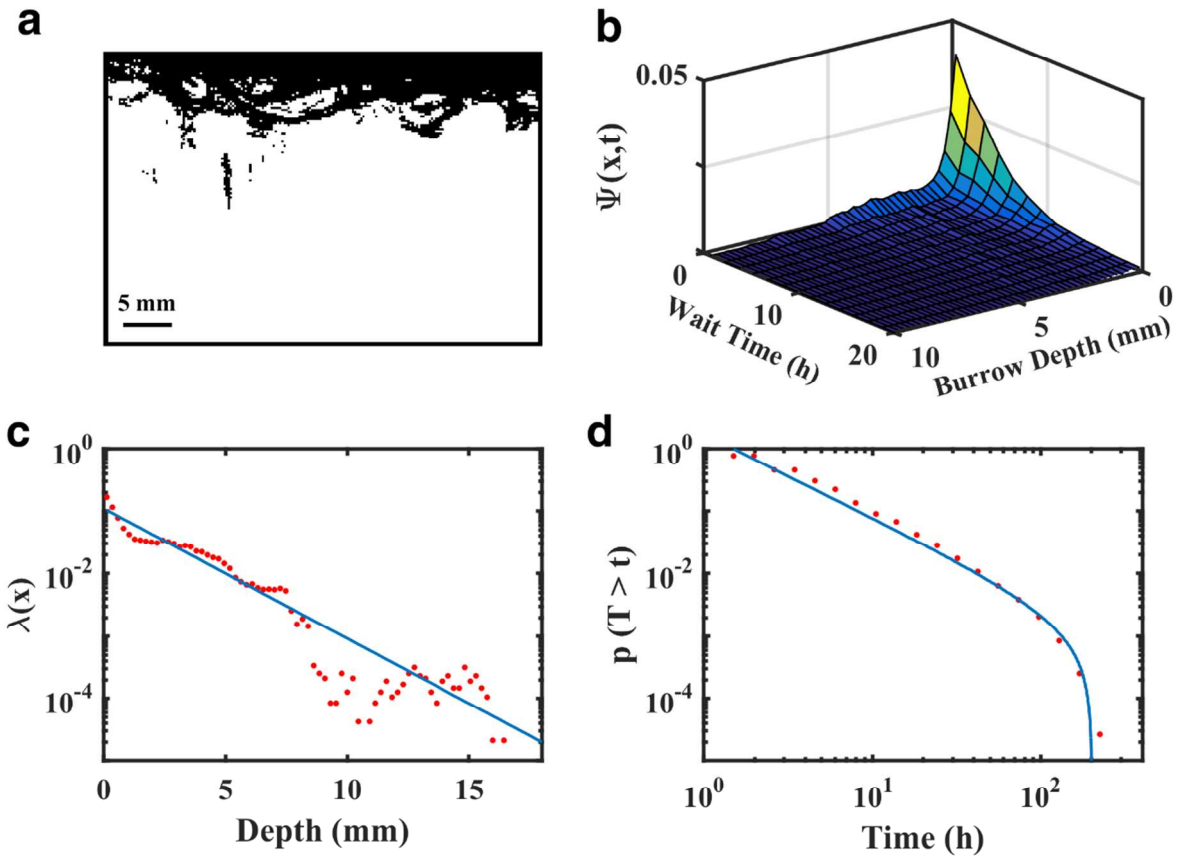

179

180 ***Figure 2****: (a) Event plot showing locations where at least one burrowing event occurred (black*
181 *pixels). Large portions of the sediment remained unworked, especially below 10 mm (white*
182 *pixels). (b) PDF of organism movements. This density was decomposed into marginal burrow-*
183 *depth and wait-time PDFs. (c) Marginal burrow-depth density with an exponential fit,*
184 $\lambda(x) \sim \gamma e^{-\gamma x}$*, where* γ *= 0.48/mm. (d) Cumulative wait-time distribution, fit to a truncated*
185 *power-law distribution,* $p(T > \tau) \sim \frac{{\tau_1}^{\beta}(\tau^{-\beta} - {\tau_2}^{-\beta})}{1-(\tau_1/\tau_2)^{\beta}}$ *, for times* $\tau_1 \ll \tau \ll \tau_2$*, where* β *is the power*
186 *law slope* [43]*. Line shows a best-fit truncated power law with* τ_1 = 1.5 h, τ_2 = 200 h, *and* β =
187 1.35.

188

Total sediment reworking (Figure 2a) and burrowing distributions (Figure 2b, c) varied with depth. By day 9, worms had reworked 86% of sediments above 5.0 mm and 10.3% of sediments between 5.0 mm and the deepest burrow (16.4 mm). Percentages increased to 90% and 13.5% by the end of the experiment. Just 3% of sediments from 10.0-16.4 mm were reworked at the experimental endpoint. The joint PDF, Ψ, shows that 56% of burrowing events were less than 5 mm with wait times less than 10 h (Figure 2b). Burrows below 10.0 mm accounted for 0.4% of all events. An average burrow depth of 2.16 mm and wait time of 0.91 d were calculated from the marginal densities.

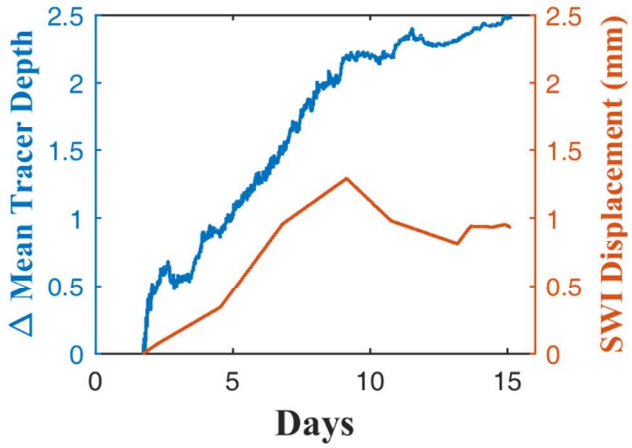

Figure 3*: Time series of mean tracer depth and SWI displacement. t = 0 is the time at which worms were introduced.*

Because sediments did not completely consolidate until 2 d after worms were introduced, we tracked the evolution of the average SWI location relative to its location when sediments finished consolidating (day 2). After consolidation the SWI height grew linearly until stabilizing at day 9 (Figure 3, red line). Time-lapse photography showed that this stabilization was primarily due to excavated sediment mounds collapsing at a rate equal to their growth (see movie S1). However, the rate of sediment reworking also decreased from 4,200 pixels/day to 3,200 pixels/day after

day 9 (24% decrease). SWI velocity was found to be 0.18 mm/d for the initial period of linear growth (days 2-9).

Fluorescent Tracer Results

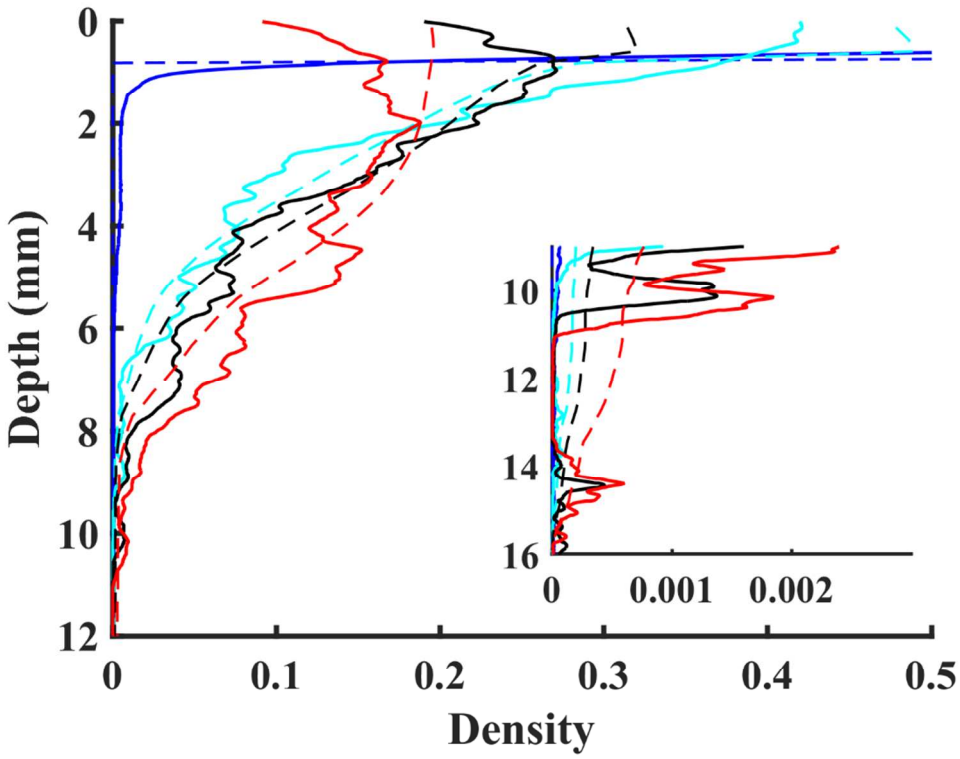

Figure 4*: Fluorescence profiles from the experiment (—) and the joint random walk model (– –) at different times; blue, cyan, black, and red lines are 0, 4, 7, and 15 d, respectively. Tracer spread rapidly from the SWI and then slowed at later times, as evidenced by the similarity between Day 7 and Day 15 profiles. Inset shows tracer profiles in deep sediments. The model captured rapid tracer propagation into deep sediment layers (below 10 mm), which could not be captured by the ADE model (results shown in Supporting Information).*

Tracer particles were rapidly mixed near the SWI (upper 5 mm) and also rapidly driven into deeper into the bed. Depth-averaged tracer concentration profiles are shown in Figure 4 for

multiple times. Profiles are characterized by a slow advection of the tracer peak, accompanied by a gradual decrease in the peak concentration and spreading of the tracer profile. Both advection and spreading of the peak slowed at day 9, and little change occurred in the profile from days 9-15. Nonlocal tracer transport was observed as early as 1.75 d, when a peak appeared at 8 mm depth. The first peak below 10 mm appeared on Day 6 (14 mm).

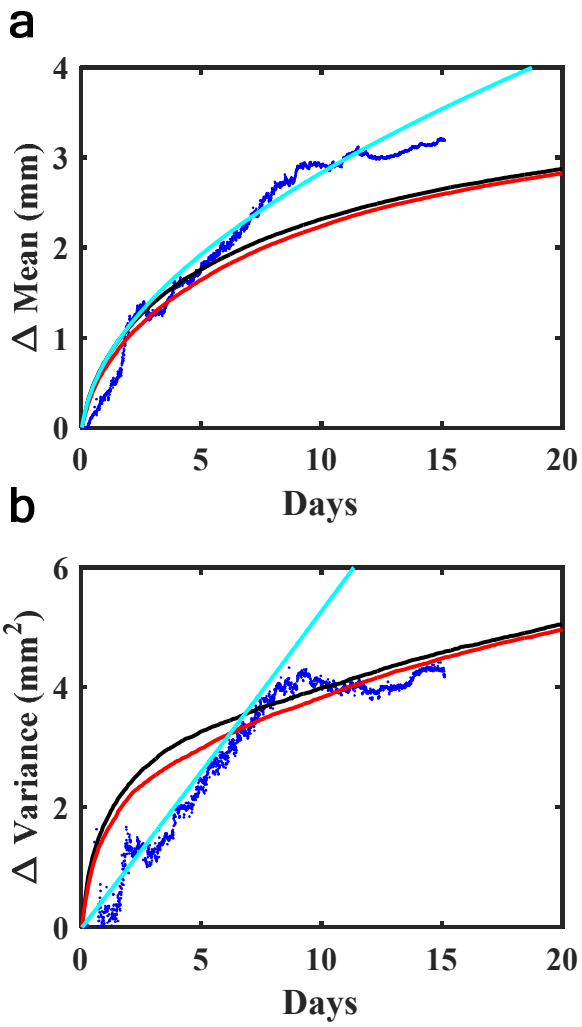

Figure 5: *Changes in tracer mean (a) and variance (b) from initial values calculated from experimental observations (blue dots) and predicted by the models (black line for coupled, red line for uncoupled, and cyan line for ADE).*

The gradual changes in advection and spreading were also reflected in the first- and second-order statistics of the profiles (Figure 5, blue dots). Both experimental statistics showed a sharp transition to slower growth rates at day 9, and this timing corresponded exactly to the transition in the SWI displacement (Figure 3). Similar trends in tracer mean and variance were observed in a replicate experiment (see Supporting Information).

Model Results

The random walk model reproduced several central features of the experimental tracer profiles, including the slow advection of the tracer peak, spreading of the peak, nonlocal transport beyond 10 mm, and rapid mixing of near-surface sediments (Figure 4). The coupled and uncoupled models performed nearly identically, which indicates that burrowing depth and frequency were largely independent. Random walk simulations captured the overall trend in both the mean and variance, but under-predicted the observed mean tracer propagation (Figure 5). However, the asymptotic rate of increase of the mean was identical between models and experiment (0.04 mm/d at day 15), indicating that the random walk model captures the asymptotic behavior over long times. Predicted and observed variance matched near the experimental endpoint, but model's rate of increase was 3 times faster than the experimental rate (0.09 mm^2/d vs 0.03 mm^2/d, averaged over 1 d).

Because the sediment redistribution time series exhibited a clear non-diffusive trend, we fit the ADE model over the initial time interval where experimental variance was linear (days 0-9). Best-fit values were $U_b = 0.052$ mm/d and $D_b = 0.73$ mm^2/d. The ADE could not adequately capture deep burrowing events at early times because this model only represents local diffusive fluxes with an inherent length support scale of $\sqrt{2D_b t}$. As a result, the ADE only predicted significant motion below 10 mm after 3.9 d (based on tracer concentration density > 1 x 10^{-4}),

254 whereas the random walk model reached this threshold over just 0.4 d because of its ability to
255 reproduce rapid, nonlocal transport events based on the observed spatial and temporal scales of
256 worm burrow events. The ADE model greatly overpredicted the mean transport at late times
257 because this model only accounts for mean transport with a time-invariant advection parameter.
258 Mixing events in the random walk model were directly related to burrowing events and, thus,
259 were appropriately restricted to the bioactive region of sediments. This enabled the random walk
260 model to more accurately capture the observed transition to slower mean transport after day 9.
261 Similarly, ADE variance increased linearly, which matched the experimental result at early times
262 (a direct consequence of the model fit) but failed to capture the transition to slower spreading
263 after day 9. This transition was captured by the random walk model owing to its direct encoding
264 of the linkage between burrowing events and sediment mixing.
265
266 DISCUSSION:
267 *Worm burrowing and sediment mixing*
268 *L. variegatus* motion was highly heterogeneous. Although this organism is commonly
269 described as an upward conveyor[37, 44], we observed several distinct behaviors, including
270 sediment excavation, particle ingestion/egestion, rapid reworking of interfacial sediments, and
271 deep burrowing. Burrows were biased to the upper 10 mm of the bed (99.6% of events), which
272 left extensive areas of the subsurface unaltered (Figure 2a). Marginal burrow-depth probabilities
273 show that the majority of depths follow an exponential PDF. However, the infrequent deep
274 burrowing events (0.4%) that rapidly transported sediments beyond 10 mm were not adequately
275 described by this PDF, and were instead super-exponential. The marginal wait-time distribution
276 contains a scale-free region from 1.5-200 h, illustrating a wide range of times between revisits to

277 a specific location. The lower limit of this distribution is expected to extend to the minute scale,
278 since we observed frequent organism movements in images taken 3 min apart. Similarly,
279 truncation at 200 h simply reflects the experiment duration, since the majority (64%) of the
280 sediments between the SWI and the deepest burrow remained unperturbed at the end of the
281 experiment.

282 Heterogeneous burrowing by *L. variegatus* resulted in anomalous sediment mixing. Deep
283 burrow events immediately delivered tracer particles well below the SWI, illustrating that these
284 very infrequent events significantly influenced the tracer distribution by transporting sediments
285 nonlocally. Low tracer concentrations below 10 mm were visible in the 1-D fluorescence profiles
286 by day 4 (Figure 4), even though worms had only reworked a small portion of these sediments:
287 only 3% of sediments between 10-16 mm depth had been reworked at the end of the experiment.
288 Mean and variance of the tracer concentration profiles increased steadily for the first 9 days of
289 the experiment (Figure 5), and then continued to increase at a slower rate thereafter. A similar
290 transition was observed in the SWI dynamics (Figure 3, red line). Time-lapse images show that
291 worms created steadily-growing mounds of sediment during the first 9 days, displacing the SWI
292 upward. Mounds collapsed after reaching a critical height and/or after disruption by worms.
293 Mound growth and collapse equilibrated at day 9, leading to stochastic variations but no net
294 increase in the SWI height after this time. The synchronous changes in tracer statistics and mean
295 SWI height suggest that sediment mixing is directly linked to mound formation on the SWI,
296 meaning propagation of particles is not only due to worm movements below the surface, but also
297 deposition of egested and excavated particles at the SWI.

298 Sediment mixing by *L. variegatus* was also time dependent. Tracer particles initially
299 propagated downward at a rate of 0.32 mm/d (Figure 5a), and propagation slowed to 0.04 mm/d

after day 9. By this time worms had already reworked 86% of sediments above 5 mm. Subsequent sediment reworking near the SWI did not substantially alter tracer distributions, since tracer particles were well mixed in this region. Ongoing burrowing deeper in the sediments controlled downward tracer propagation at late times. The fraction of sediments reworked between 5-16 mm increased by 30% after day 9.

These results show that a minimum of several weeks are needed before a pulse of particles is well mixed in the zone of *L. variegatus* activity, which is an important consideration for sediment biogeochemistry[7, 15, 45, 46]. In particular, our findings suggest that heterogeneous sediment reworking by bioturbating organisms strongly influences the timescale of response to natural and engineered perturbations. The infrequency of nonlocal bioturbation events leaves large areas of deep sediments unmixed for long periods of time, limiting interaction between new and pre-existing particles at these depths. This is expected to limit the timescale of response to sediment amendments for site remediation that require close contact between introduced particles and contaminated sediments[1 47-50]. Nonlocal transport also can mobilize contaminated sediments from depth while effectively bypassing regions of sediment capping or amendment. The approach presented here can be used to predict conditions under which introduced particles can be simply deposited on the SWI vs. conditions that require active mixing to ensure adequate contact with underlying contaminated sediments.

Sediment Transport Model

Our random walk model uniquely relates biophysical information to sediment mixing, utilizing statistics of organism motion acquired through a novel direct-visualization approach. The model's use of burrow statistics as a proxy for organism motion directly links sediment transport to the most relevant governing process (burrowing), as opposed to commonly-used bioturbation

models that represent transport with assumed system-scale descriptive parameters, e.g., biodiffusion coefficient. The model specifically relates observations of burrow formation to sediment motion over all relevant spatial and temporal scales, which distinguishes it from local continuum models that are inherently limited to frequent small-scale motions. The classical biodiffusion model adequately captures the effects of frequent, local mixing events near the SWI, but does not represent intermittent tracer displacements to deep sediments or the associated transition from fast mixing of surficial sediments to slower mixing of deeper sediments. Models with a depth-dependent diffusion coefficient can improve fits to tracer data[13, 51], but they inherently cannot represent nonlocal transport and are non-transferrable because they are not explicitly related to the underlying motion processes. Conveyor-feeding models explicitly incorporate nonlocal particle displacements[20, 24], but also do not capture the full range of sediment motion because they impose restrictions on the scales over which these displacements occur.

The random walk model presented here directly represents the effects of macroscopic organism motions. Application of the model to specific behavioral classes of organisms requires the development of rules that relate organism motion to sediment redistribution. For surface deposit feeders and other species regarded as true biodiffusors[28, 52, 53], organism motions homogenize sediments locally, yielding the classical biodiffusion model as an outcome. However, the general approach proposed here can represent sediment mixing caused by a much wider range of organism behaviors in a unified, fundamental theoretical framework. The specific transport rule developed for the oligochaete *Lumbriculus variegatus* is based on known behavior of the organism (head-down deposit feeder), as well as direct observations of burrowing events, mound formation, and tracer redistribution within the sediments. Burrowing statistics were

obtained via direct visualization, and the fraction of sediments delivered to the SWI was obtained by measuring the accumulation of sediments on the SWI caused by burrow excavation and sediment egestion. The model provides a parsimonious description of key sediment mixing outcomes that are not captured by conventional biodiffusion models, including time-dependent burial and spreading of the tracer peak, long-term trends in the mean and variance of the tracer concentration profiles, and nonlocal mixing in deep sediments (Figure 4). This sediment redistribution rule is expected to apply to the general class of deposit feeding organisms historically considered surface feeders or conveyor-belt feeders[24, 54-56], comprising many oligochaete and polychaete species[57-60], as well as gallery diffusers (e.g., *Nereis diversicolor*) and predators (e.g., *Nephtys caeca*) that mix sediments diffusively near the SWI and nonlocally at depth[52, 60-62]. The transport rule can be reformulated to represent other types of organism behavior. The model assumes that all sediments are equally likely to be remobilized, which is not expected to be the case for all organisms or sediments. For example, the oligochaete *Tubifex tubifex* is generally considered an upward conveyor (nonlocal transport) of fine (< 63 μm) sediments, but does not transport larger particles[63].

The model also assumes that all burrow events are independent and stationary (i.e., time invariant), implying that organism numbers and behavior do not change over time. These limitations are expected to be most severe for prediction of deeper and longer-term sediment mixing. For example, increased probability of organism revisits to existing burrows (as opposed to the formation of new burrows) and decreases in organism numbers over time will both lead to decreased mixing of deep sediments at late times. Further model generalization is therefore required to represent cases where burrowing activity varies with time. Future research efforts should explore extensions to represent nonstationarity and correlations related to time-varying

369 worm populations and other population- and community-level changes in the benthic ecosystem,
370 including species-pair interactions[64, 65], burrow network/gallery formation[66, 67], and behavioral
371 changes due to environmental cues (e.g., toxicity, temperature)[28, 68, 69].
372
373 *Environmental Implications*
374 The combined experimental and modeling approach introduced here simplifies model
375 parameterization and improves transferability by relating input parameters to the most critical
376 measurable system attributes. Future research is needed to elucidate the specific roles of
377 sediment reworking and other biologically-mediated transport mechanisms (e.g., solute exchange
378 via bioirrigation[3]) in sediment biogeochemistry[62, 70, 71]. These efforts will inform the proper
379 coupling between transport and biogeochemical models—a necessary step for predicting
380 responses to large-scale environmental pressures and designing successful site remediation
381 strategies[72, 73].
382
383 AUTHOR INFORMATION
384 **Corresponding Author**
385 *E-mail: kevinroche2012@u.northwestern.edu; tel: 219-869-5368; fax: 847-491-4011
386
387 ACKNOWLEDGMENTS
388 We thank Liliana Hernandez-Gonzalez for her assistance with sediment collection and
389 experiment setup. This research was supported by the SERPD program (ER-1745). K.R.R. was
390 supported by a NSF Graduate Research Fellowship; M.X. was supported by SERDP Grant ER-
391 1745. T.A. gratefully acknowledges support by the Portuguese Foundation for Science and
392 Technology (FCT) under Grant SFRH/BD/89488/2012. D.B. was supported by NSF Grants
393 EAR-1344280, EAR-1351625, and EAR-1417264. A.F.A. and A.I.P. were supported by U.S.
394 NSF Grant EAR-1344280.
395 ASSOCIATED CONTENT

Supporting Information.

Additional time-lapse videos and image processing algorithms, as noted in the text, are available free of charge via the Internet at http://pubs.acs.org.

REFERENCES

1. Thibodeaux, L. J.; Bierman, V. J., The bioturbation-driven chemical release process. *Environmental Science & Technology* **2003,** *37*, (13), 252A-258A.
2. Meysman, F. J.; Middelburg, J. J.; Heip, C. H., Bioturbation: a fresh look at Darwin's last idea. *Trends in Ecology & Evolution* **2006,** *21*, (12), 688-695.
3. Kristensen, E.; Penha-Lopes, G.; Delefosse, M.; Valdemarsen, T.; Quintana, C. O.; Banta, G. T., What is bioturbation? The need for a precise definition for fauna in aquatic sciences. *Marine Ecology Progress Series* **2011,** *446*, 285-302.
4. Lehmann, M. F.; Bernasconi, S. M.; Barbieri, A.; McKenzie, J. A., Preservation of organic matter and alteration of its carbon and nitrogen isotope composition during simulated and in situ early sedimentary diagenesis. *Geochimica et Cosmochimica Acta* **2002,** *66*, (20), 3573-3584.
5. Canavan, R. W.; Slomp, C. P.; Jourabchi, P.; Van Cappellen, P.; Laverman, A. M.; van den Berg, G. A., Organic matter mineralization in sediment of a coastal freshwater lake and response to salinization. *Geochimica et Cosmochimica Acta* **2006,** *70*, (11), 2836-2855.
6. Thomsen, U.; Thamdrup, B.; Stahl, D. A.; Canfield, D. E., Pathways of organic carbon oxidation in a deep lacustrine sediment, Lake Michigan. *Limnology and Oceanography* **2004,** *49*, (6), 2046-2057.
7. Remaili, T. M.; Simpson, S. L.; Amato, E. D.; Spadaro, D. A.; Jarolimek, C. V.; Jolley, D. F., The impact of sediment bioturbation by secondary organisms on metal bioavailability, bioaccumulation and toxicity to target organisms in benthic bioassays: Implications for sediment quality assessment. *Environmental Pollution* **2016,** *208, Part B*, 590-599.
8. Simpson, S. L.; Ward, D.; Strom, D.; Jolley, D. F., Oxidation of acid-volatile sulfide in surface sediments increases the release and toxicity of copper to the benthic amphipod Melita plumulosa. *Chemosphere* **2012,** *88*, (8), 953-961.
9. Ciutat, A.; Boudou, A., Bioturbation effects on cadmium and zinc transfers from a contaminated sediment and on metal bioavailability to benthic bivalves. *Environmental Toxicology and Chemistry* **2003,** *22*, (7), 1574-1581.
10. Sundelin, B.; Eriksson, A.-K., Mobility and bioavailability of trace metals in sulfidic coastal sediments. *Environmental Toxicology and Chemistry* **2001,** *20*, (4), 748-756.
11. Phipps, G. L.; Ankley, G. T.; Benoit, D. A.; Mattson, V. R., Use of the aquatic oligochaete Lumbriculus variegatus for assessing the toxicity and bioaccumulation of sediment-associated contaminants. *Environmental Toxicology and Chemistry* **1993,** *12*, (2), 269-279.
12. Bessinger, B. A.; Vlassopoulos, D.; Serrano, S.; O'Day, P. A., Reactive Transport Modeling of Subaqueous Sediment Caps and Implications for the Long-Term Fate of Arsenic, Mercury, and Methylmercury. *Aquatic Geochemistry* **2012,** *18*, (4), 297-326.

13. Boudreau, B. P., The mathematics of early diagenesis: From worms to waves. *Reviews of Geophysics* **2000,** *38*, (3), 389-416.
14. Lampert, D. J.; Reible, D., An Analytical Modeling Approach for Evaluation of Capping of Contaminated Sediments. *Soil and Sediment Contamination: An International Journal* **2009,** *18*, (4), 470-488.
15. Lin, D.; Cho, Y.-M.; Werner, D.; Luthy, R. G., Bioturbation Delays Attenuation of DDT by Clean Sediment Cap but Promotes Sequestration by Thin-Layered Activated Carbon. *Environ Sci Technol* **2014,** *48*, (2), 1175-1183.
16. Berner, R. A., *Early diagenesis: A theoretical approach*. Princeton University Press: 1980.
17. Goldberg, E. D.; Koide, M., Geochronological studies of deep sea sediments by the ionium/thorium method. *Geochimica et Cosmochimica Acta* **1962,** *26*, (3), 417-450.
18. Guinasso, N. L.; Schink, D. R., Quantitative estimates of biological mixing rates in abyssal sediments. *Journal of Geophysical Research* **1975,** *80*, (21), 3032-3043.
19. Thibodeaux, L. J.; Valsaraj, K. T.; Reible, D. D., Bioturbation-driven transport of hydrophobic organic contaminants from bed sediment. *Environmental engineering science* **2001,** *18*, (4), 215-223.
20. Boudreau, B. P., Mathematics of tracer mixing in sediments; I, Spatially-dependent, diffusive mixing. *American Journal of Science* **1986,** *286*, (3), 161-198.
21. Meysman, F. J.; Boudreau, B. P.; Middelburg, J. J., When and why does bioturbation lead to diffusive mixing? *Journal of Marine Research* **2010,** *68*, (6), 881-920.
22. Metzler, R.; Klafter, J., The random walk's guide to anomalous diffusion: a fractional dynamics approach. *Physics Reports* **2000,** *339*, (1), 1-77.
23. Zhang, Y.; Meerschaert, M. M.; Packman, A. I., Linking fluvial bed sediment transport across scales. *Geophysical Research Letters* **2012,** *39*, (20), L20404.
24. Robbins, J. A., A model for particle-selective transport of tracers in sediments with conveyor belt deposit feeders. *Journal of Geophysical Research: Oceans (1978--2012)* **1986,** *91*, (C7), 8542-8558.
25. Boudreau, B. P., Mathematics of tracer mixing in sediments: II. Nonlocal mixing and biological conveyor-belt phenomena. *Am. J. Sci* **1986,** *286*, (3), 199-238.
26. François, F.; Poggiale, J.-C.; Durbec, J.-P.; Stora, G., A new approach for the modelling of sediment reworking induced by a macrobenthic community. *Acta Biotheoretica* **1997,** *45*, (3-4), 295-319.
27. Meysman, F. J.; Malyuga, V. S.; Boudreau, B. P.; Middelburg, J. J., A generalized stochastic approach to particle dispersal in soils and sediments. *Geochimica et Cosmochimica Acta* **2008,** *72*, (14), 3460-3478.
28. Maire, O.; Duchêne, J.; Grémare, A.; Malyuga, V.; Meysman, F., A comparison of sediment reworking rates by the surface deposit-feeding bivalve Abra ovata during summertime and wintertime, with a comparison between two models of sediment reworking. *Journal of Experimental Marine Biology and Ecology* **2007,** *343*, (1), 21-36.
29. Bernard, G.; Grémare, A.; Maire, O.; Lecroart, P.; Meysman, F. J.; Ciutat, A.; Deflandre, B.; Duchêne, J. C., Experimental assessment of particle mixing fingerprints in the deposit-feeding bivalve Abra alba (Wood). *Journal of Marine Research* **2012,** *70*, (5), 689-718.
30. Maire, O.; Lecroart, P.; Meysman, F.; Rosenberg, R.; Duchene, J.; Grémare, A., Quantification of sediment reworking rates in bioturbation research: a review. *Aquatic Biology* **2008,** *2*, 219-238.

31. Meysman, F. J.; Malyuga, V.; Boudreau, B. P.; Middelburg, J., Quantifying particle dispersal in aquatic sediments at short time scales: model selection. *Aquatic Biology* **2008,** *2*, 239-254.
32. Lauritsen, D. D.; Mozley, S. C.; White, D. S., Distribution of Oligochaetes in Lake Michigan and Comments on Their use as Indices of Pollution. *Journal of Great Lakes Research* **1985,** *11*, (1), 67-76.
33. Spencer, D. R., The Aquatic Oligochaeta of the St. Lawrence Great Lakes Region. In *Aquatic Oligochaete Biology*, Brinkhurst, R. O.; Cook, D. G., Eds. Springer US: Boston, MA, 1980; pp 115-164.
34. Timm, T., Distribution of aquatic oligochaetes. In *Aquatic Oligochaete Biology*, Springer: 1980; pp 55-77.
35. Xie, M. W.; Jarrett, B. A.; Da Silva-Cadoux, C.; Fetters, K. J.; Burton, G. A.; Gaillard, J. F.; Packman, A. I., Coupled Effects of Hydrodynamics and Biogeochemistry on Zn Mobility and Speciation in Highly Contaminated Sediments. *Environ Sci Technol* **2015,** *49*, (9), 5346-5353.
36. Smith, M. E.; Lazorchak, J. M.; Herrin, L. E.; Brewer-Swartz, S.; Thoeny, W. T., A reformulated, reconstituted water for testing the freshwater amphipod, Hyalella azteca. *Environmental Toxicology and Chemistry* **1997,** *16*, (6), 1229-1233
37. Landrum, P.; Gedeon, M.; Burton, G.; Greenberg, M.; Rowland, C., Biological responses of Lumbriculus variegatus exposed to fluoranthene-spiked sediment. *Archives of environmental contamination and toxicology* **2002,** *42*, (3), 292-302.
38. Sauter, G.; Güde, H., Influence of grain size on the distribution of tubificid oligochaete species. *Hydrobiologia* **1996,** *334*, (1), 97-101.
39. Cook, D. G.; Johnson, M. G., Benthic Macroinvertebrates of the St. Lawrence Great Lakes. *Journal of the Fisheries Research Board of Canada* **1974,** *31*, (5), 763-782.
40. Brinkhurst, R. O., Distribution and Abundance of Tubificid (Oligochaeta) Species in Toronto Harbour, Lake Ontario. *Journal of the Fisheries Research Board of Canada* **1970,** *27*, (11), 1961-1969.
41. Polyanin, A. D.; Nazaikinskii, V. E., *Handbook of Linear Partial Differential Equations for Engineers and Scientists*. CRC press: 2016.
42. Montgomery, D. C.; Runger, G. C., *Applied Statistics and Probability for Engineers*. John Wiley & Sons: 2010.
43. Aban, I. B.; Meerschaert, M. M.; Panorska, A. K., Parameter Estimation for the Truncated Pareto Distribution. *Journal of the American Statistical Association* **2006,** *101*, (473), 270-277.
44. Lick, W., The Sediment-Water Flux of HOCs Due to "Diffusion" or Is There a Well-Mixed Layer? If There Is, Does It Matter? *Environ Sci Technol* **2006,** *40*, (18), 5610-5617.
45. Koelmans, A. A.; Jonker, M. T. O., Effects of black carbon on bioturbation-induced benthic fluxes of polychlorinated biphenyls. *Chemosphere* **2011,** *84*, (8), 1150 - 1157.
46. Kupryianchyk, D.; Noori, A.; Rakowska, M. I.; Grotenhuis, J. T. C.; Koelmans, A. A., Bioturbation and Dissolved Organic Matter Enhance Contaminant Fluxes from Sediment Treated with Powdered and Granular Activated Carbon. *Environ Sci Technol* **2013,** *47*, (10), 5092-5100.
47. Millward, R. N.; Bridges, T. S.; Ghosh, U.; Zimmerman, J. R.; Luthy, R. G., Addition of Activated Carbon to Sediments to Reduce PCB Bioaccumulation by a Polychaete (Neanthes arenaceodentata) and an Amphipod (Leptocheirus plumulosus). *Environ Sci Technol* **2005,** *39*, (8), 2880-2887.

527 48. Dąbrowski, A.; Podkościelny, P.; Hubicki, Z.; Barczak, M., Adsorption of phenolic
528 compounds by activated carbon—a critical review. *Chemosphere* **2005,** *58*, (8), 1049-1070.
529 49. Luthy, R. G.; Aiken, G. R.; Brusseau, M. L.; Cunningham, S. D.; Gschwend, P. M.;
530 Pignatello, J. J.; Reinhard, M.; Traina, S. J.; Weber, W. J.; Westall, J. C., Sequestration of
531 Hydrophobic Organic Contaminants by Geosorbents. *Environ Sci Technol* **1997,** *31*, (12), 3341-
532 3347.
533 50. Kosian, P. A.; West, C. W.; Pasha, M. S.; Cox, J. S.; Mount, D. R.; Huggett, R. J.;
534 Ankley, G. T., Use of nonpolar resin for reduction of fluoranthene bioavailability in sediment.
535 *Environmental Toxicology and Chemistry* **1999,** *18*, (2), 201-206.
536 51. Christensen, E. R., A model for radionuclides in sediments influenced by mixing and
537 compaction. *Journal of Geophysical Research: Oceans* **1982,** *87*, (C1), 566-572.
538 52. Piot, A.; Rochon, A.; Stora, G.; Desrosiers, G., Experimental study on the influence of
539 bioturbation performed by Nephtys caeca (Fabricius) and Nereis virens (Sars) annelidae on the
540 distribution of dinoflagellate cysts in the sediment. *Journal of Experimental Marine Biology and*
541 *Ecology* **2008,** *359*, (2), 92-101.
542 53. Robbins, J. A.; McCall, P. L.; Fisher, J. B.; Krezoski, J. R., Effect of deposit feeders on
543 migration of137Cs in lake sediments. *Earth and Planetary Science Letters* **1979,** *42*, (2), 277-
544 287.
545 54. Rhoads, D., Organism-sediment relations on the muddy sea floor. Oceanogr. *Mar. Biol.*
546 *Ann. Rev.* **1974,** *12*, 263-300.
547 55. Powell, E. N., Particle size selection and sediment reworking in a funnel feeder,
548 Leptosynapta tenuis (Holothuroidea, Synaptidae). *Internationale Revue der gesamten*
549 *Hydrobiologie und Hydrographie* **1977,** *62*, (3), 385-408.
550 56. Kristensen, E.; Penha-Lopes, G.; Delefosse, M.; Valdemarsen, T.; Quintana, C. O.;
551 Banta, G. T., What is bioturbation? The need for a precise definition for fauna in aquatic
552 sciences. *Marine Ecology Progress Series* **2012,** *446*, 285-302.
553 57. Lopez, G. R.; Levinton, J. S., Ecology of Deposit-Feeding Animals in Marine Sediments.
554 *The Quarterly Review of Biology* **1987,** *62*, (3), 235-260.
555 58. McCall, P. L.; Tevesz, M. J., *The effects of benthos on physical properties of freshwater*
556 *sediments*. Springer: 1982.
557 59. Hutchings, P., Biodiversity and functioning of polychaetes in benthic sediments.
558 *Biodiversity & Conservation* **1998,** *7*, (9), 1133-1145.
559 60. Gérino, M.; Stora, G.; François-Carcaillet, F.; Gilbert, F.; Poggiale, J.-C.; Mermillod-
560 Blondin, F.; Desrosiers, G.; Vervier, P., Macro-invertebrate functional groups in freshwater and
561 marine sediments: a common mechanistic classification. *Vie et Milieu* **2003,** *53*, (4), 221-231.
562 61. François, F.; Gerino, M.; Stora, G.; Durbec, J.-P.; Poggiale, J.-C., Functional approach to
563 sediment reworking by gallery-forming macrobenthic organisms: modeling and application with
564 the polychaete Nereis diversicolor. *Marine Ecology Progress Series* **2002,** *229*, 127-136.
565 62. Pischedda, L.; Poggiale, J.-C.; Cuny, P.; Gilbert, F., Imaging oxygen distribution in
566 marine sediments. The importance of bioturbation and sediment heterogeneity. *Acta*
567 *biotheoretica* **2008,** *56*, (1-2), 123-135.
568 63. Mermillod-Blondin, F.; Gérino, M.; Degrange, V.; Lensi, R.; Chassé, J.-L.; Rard, M.;
569 Châtelliers, M. C. d., Testing the functional redundancy of Limnodrilus and Tubifex
570 (Oligochaeta, Tubificidae) in hyporheic sediments: an experimental study in microcosms.
571 *Canadian Journal of Fisheries and Aquatic Sciences* **2001,** *58*, (9), 1747-1759.

64. Preisser, E. L.; Bolnick, D. I.; Benard, M. F., Scared to Death? The Effects of Intimidation and Consumption in Predator–Prey Interactions. *Ecology* **2005,** *86*, (2), 501-509.
65. Kaster, J. L., Observations of predator-prey interaction on dispersal of an oligochaete prey, Limnodrilus hoffmeisteri. *Hydrobiologia 180*, (1), 191-193.
66. Ziebis, W.; Forster, S.; Huettel, M.; Jørgensen, B., Complex burrows of the mud shrimp Callianassa truncata and their geochemical impact in the sea bed. *Nature* **1996,** *382*, (6592), 619-622.
67. Nogaro, G.; Mermillod-Blondin, F.; FranÇOis- Carcaillet, F.; Gaudet, J.-P.; Lafont, M.; Gibert, J., Invertebrate bioturbation can reduce the clogging of sediment: an experimental study using infiltration sediment columns. *Freshwater Biology* **2006,** *51*, (8), 1458-1473.
68. Sardo, A. M.; Soares, A. M. V. M., Can behavioural responses of Lumbriculus variegatus (Oligochaeta) assess sediment toxicity? A case study with sediments exposed to acid mine drainage. *Environmental Pollution* **2010,** *158*, (2), 636-640.
69. Landrum, P. F.; Leppänen, M.; Robinson, S. D.; Gossiaux, D. C.; Burton, G. A.; Greenberg, M.; Kukkonen, J. V. K.; Eadie, B. J.; Lansing, M. B., Effect of 3,4,3,4'-tetrachlorobiphenyl on the reworking behavior of Lumbriculus variegatus exposed to contaminated sediment. *Environmental Toxicology and Chemistry* **2004,** *23*, (1), 178-186.
70. Volkenborn, N.; Polerecky, L.; Wethey, D.; Woodin, S., Oscillatory porewater bioadvection in marine sediments induced by hydraulic activities of Arenicola marina. *Limnology and oceanography* **2010,** *55*, (3), 1231.
71. Mermillod-Blondin, F.; Rosenberg, R.; François-Carcaillet, F.; Norling, K.; Mauclaire, L., Influence of bioturbation by three benthic infaunal species on microbial communities and biogeochemical processes in marine sediment. *Aquatic Microbial Ecology* **2004,** *36*, (3), 271-284.
72. Burton, G. A.; Johnston, E. L., Assessing contaminated sediments in the context of multiple stressors. *Environmental Toxicology and Chemistry* **2010,** *29*, (12), 2625-2643.
73. Lohrer, A. M.; Thrush, S. F.; Gibbs, M. M., Bioturbators enhance ecosystem function through complex biogeochemical interactions. *Nature* **2004,** *431*, (7012), 1092-1095.

TOC Art